Flow, Turbulence and Combustion **72:** 161–179, 2004.

The First Turbulence and First Fossil Turbulence

CARL H. GIBSON
Departments of Mechanical and Aerospace Engineering, and Scripps Institution of Oceanography, Center for Astrophysics and Space Sciences, University of California at San Diego, La Jolla, CA 92093-0411; E-mail: cgibson@ucsd.edu

Received 18 May 2003; accepted in revised form 24 March 2004

Abstract. A model is proposed connecting turbulence, fossil turbulence and the big-bang origin of the universe. While details are incomplete, the model is consistent with our knowledge of these processes and is supported by observations. Turbulence arises in a hot big-bang quantum gravitational dynamics scenario at Planck scales. Chaotic, eddy-like motions produce an exothermic Planck particle cascade from 10^{-35} m at 10^{32} K to 10^{8} larger, 10^{4} cooler, quark–gluon scales. A Planck–Kerr instability gives high Reynolds number (Re $\sim 10^{6}$) turbulent combustion, space-time-energy-entropy and turbulent mixing. Batchelor–Obukhov–Corrsin turbulent-temperature fluctuations are preserved as the first fossil turbulence by inflation stretching the patterns beyond the horizon ct of causal connection faster than light speed c in time $t \sim 10^{-33}$ sec. Fossil big-bang temperature turbulence reenters the horizon and imprints nucleosynthesis of H–He densities that seed fragmentation by gravity at 10^{12} s in the low Reynolds number plasma before its transition to gas at $t \sim 10^{13}$ s and $T \sim 3000$ K. Multiscaling coefficients of the cosmic microwave background (CMB) temperature anisotropies closely match those for high Reynolds number turbulence, Bershadskii, A. and Sreenivasan, K.R., *Phys. Lett. A* **299** (2002) 149–152; Bershadskii, A. and Sreenivasan, K.R., *Phys. Lett. A* **319** (2003) 21–23. CMB spectra support the interpretation that big-bang turbulence fossils triggered fragmentation of the viscous plasma at supercluster to galaxy mass scales from 10^{46} to 10^{42} kg, Gibson, C.H., *Appl. Mech. Rev.* **49** (5) (1996) 299–315; Gibson, C.H., *J. Fluids Eng.* **122** (2000) 830–835; Gibson, C.H., *Combust. Sci. Technol.* (2004, to be published).

Key words: turbulence, fossil turbulence, cosmology, hydrogravitational structure formation, dark matter

1. Introduction

Turbulent motions, turbulent mixing, turbulent diffusion and fossil turbulence processes are crucial to the evolution of natural fluids such as the ocean and atmosphere. However, because the conservation equations for turbulence are nonlinear and because no systematic method exists for solving nonlinear equations, turbulence is often cited as the most important unsolved problem of classical physics. Standard cosmologies of the primordial universe assume collisionless, ideal fluids and make little or no reference to turbulence or real fluid behavior. Thus, many predictions of these standard cosmologies are unreliable.

A variety of definitions of turbulence may be found in the literature. Even the direction of the turbulence cascade is controversial. The present paper uses a narrow

Kolmogorovian definition that limits both the direction of the turbulence cascade and the dominant force [10]. The definition is based on the nonlinear term $\vec{v} \times \vec{\omega}$ in the Bernoulli form of the momentum conservation equations called the inertial vortex force, where $\vec{v}$ is the velocity and $\vec{\omega} \equiv \nabla \times \vec{v}$ is the vorticity. By definition, turbulence always starts at universal critical Reynolds number Kolmogorov scales and cascades to larger scales until constrained by boundaries, other forces or by the scale of causal connection *ct*. Inertial vortex forces of big-bang turbulence must overcome large gravitational forces that arise at 10^{-35} m Planck (Kolmogorov) scales of the big-bang. Planck temperatures 10^{32} K are too high for quark–gluons. Gluons increase the viscosity and dampen the turbulence cascade when the 10^{28} K quark–gluon temperature is reached by the expanding universe. Big-bang turbulence (BBT) requires a turbulence cascade from small scales to large. Many turbulence definitions assume the reverse.

Self-gravitational fragmentation can be seeded by BBT fossils when viscous or weak turbulence Schwarz scales become less than *ct* [11]. Schwarz scales of self-gravitation are equivalent to Ozmidov–Monin–Obukhov scales that describe buoyancy limited flows. In the density stratified ocean and atmosphere, vertical buoyancy forces match inertial vortex forces of growing turbulence to produce Ozmidov-scale fossil turbulence patches at a universal critical Froude number [12]. Fossil turbulence waves are radiated near-vertically to transport momentum, energy and information to other layers, where more turbulence and fossilization occurs [20]. Similarly, self-gravitational turbulence fossilization processes are manifested in the Schwarz length and mass scales of hydro-gravitational structure formation in astrophysics and cosmology [11, 13]. The presently proposed Planck–Kerr quantum gravitational instability and expansion of the hot big-bang universe at Planck scales matches our turbulence definition and thus is the first turbulence.

Random fluctuations produced at a later time by complex hydromagnetic forces [5] are not turbulence by our definition and do not have the unique physical effects of turbulence such as turbulent mixing and fossilization. Electromagnetic forces and low-mass or mass-less momentum transport particles (bosons) that appear at cooler (e.g., weak-force freeze-out) temperatures tend to dampen rather than cause strong turbulence. Whatever magnetic fields appear due to the inhomogeneities of nucleosynthesis in the first 3 min., Weinberg [32], will be stretched to small strength values by the continued expansion of the universe.

A distinctive property of turbulence is the irreversibility of its effects, leading to the concept of fossil turbulence. Linear waves come and go without leaving a trace, but turbulence and turbulent mixing produce unique and persistent fingerprints termed fossil turbulence from which previous hydrophysical parameters like dissipation rates, viscosities and diffusivities may be extracted by the process of hydropaleontology [12, 20]. Information preserved by fossil turbulence is valuable in interpreting oceanographic, atmospheric and cosmological measurements, where little or no possibility exists to detect the turbulence in its active state [13]. Turbulence irreversibility is proposed as the likely mechanism by which the highly

reversible quantum vacuum oscillations of the quantum gravitational dynamics (QGD) epoch produced the first entropy. Turbulence irreversibility is reflected in the persistence of turbulence fossils.

A variety of observations argue for a turbulence beginning of the universe. The most obvious is the scrambled homogeneity seen in Hubble Space Telescope (HST) images of galaxies in all directions at distances $\sim ct$, which locates these objects outside each other's horizons; that is, their length scales of causal connection. A sufficiently powerful turbulent big-bang preceding a superluminal inflation of space explains both puzzles. From Einstein's GR equations, space-time expands due to negative pressures such as the BBT Reynolds stress. BBT mixing and inflation give the random energy density seeds required to trigger nucleosynthesis, gravitational structure formation and the chaotic lognormal galaxy density observed at scales larger than ct.

Compelling evidence for a strong-turbulence beginning of the universe is provided by statistical parameters of the cosmic microwave background (CMB) observations. The first CMB observations from the 1989 COBE (cosmic background experiment) satellite revealed temperature anomalies $\delta T/T \sim 10^{-5}$. This is three orders of magnitude smaller than $\delta T/T \sim 10^{-2}$ expected for a strong-turbulence plasma, showing that gravitational structure formation processes must have inhibited the strong turbulence that would otherwise have developed from the kinetic energy of the expanding universe [11, 13]. The smallest ancient stars and dense spherical symmetry of globular star clusters observed in all galaxies reflects the homogeneous weak turbulence or nonturbulence of the primordial gas emerging from the plasma epoch at 300,000 yr. Multiscaling structure-function parameters of the CMB temperature anomalies closely match those of strong turbulence at length scales outside the CMB horizon [3, 4]. Photon viscosities of the plasma epoch are too large to permit strong turbulence [13]. Thus, we must explore strong-turbulence mechanisms of the big-bang itself.

The present paper presents narrow definitions of turbulence and fossil turbulence that serve to describe the behavior of conventional natural fluids, and then considers the application of these definitions to a BBT model. The predictions of the model are then compared to statistical parameters of the CMB from observations and calculations by a variety of authors using microwave telescopes on the ground, on balloons and in space.

2. A Narrow Definition of Turbulence

Webster's dictionary defines a turbulent flow as one in which the velocity at a given point varies erratically in magnitude and direction. This definition is perhaps the one most commonly used in the fields of fluid mechanics, magnetohydrodynamics, oceanography and atmospheric sciences. However, difficulties with such a broad definition of turbulence arise in its application. Viscous sublayer flows have random velocities because their boundary conditions are random, but are recognized

as nonturbulent because their Reynolds numbers are subcritical. Oceanic and atmospheric flows have a random component, but are dominated by buoyancy or Coriolis forces at large scales and may be decomposed into classes of nonturbulent linear-wave motions because their Froude and Rossby numbers are subcritical even though their Reynolds numbers are supercritical. Several oscillations in magnetohydrodynamic flows are chaotic and called turbulent but might be considered nonturbulent in other branches of fluid mechanics. For the wide range of flows that occur in nature, we need a narrow definition of turbulence that is length scale dependent and has only one nonlinear force that dominates all other forces within the turbulent range of scales.

Standard, broadly defined turbulence excludes the simple, two-parameter, turbulent universal similarity hypothesized by Kolmogorov with length scale $L_K = (\nu^3/\varepsilon)^{1/4}$ and time scale $T_K = (\nu/\varepsilon)^{1/2}$, where ν is the kinematic viscosity of the fluid and ε is the viscous dissipation rate of kinetic energy. It also excludes universal similarity of turbulent mixing [7, 8]. Kolmogorov and Batchelor–Obukhov–Corrsin universal similarity of low-order statistical parameters such as velocity and temperature spectra and lognormal intermittency constants have been observed in all turbulent flows tested [10].

Our narrow turbulence definition suggests the inertial vortex force per unit mass $\vec{v} \times \vec{\omega}$ is the universal nonlinear force that causes turbulence and the turbulence cascade, where $\vec{v}$ is the velocity and $\vec{\omega} \equiv \nabla \times \vec{v}$ is the vorticity. This is the force that causes baseballs to curve, airplanes and birds to fly and turbulence eddies to appear at Kolmogorov scales and cascade to larger (Obukhov) energy scales. It arises in the conservation of momentum equation written in the form

$$\frac{\partial \vec{v}}{\partial t} = -\nabla B + \vec{v} \times \vec{\omega} + \vec{F}_b + \vec{F}_C + \vec{F}_\nu + \cdots \tag{1}$$

where B is the Bernoulli group of mechanical energy terms $p/\rho + v^2/2 + gz$, p is the pressure, ρ is the density, g is the acceleration of gravity, z is the distance above a reference level, $\vec{F}_b$ is the buoyancy force, $\vec{F}_C$ is the Coriolis force, $\vec{F}_\nu$is the viscous force, and other forces are neglected. The Froude, Rossby and Reynolds numbers i.e., Fr, Ro and Re are ratios of $\vec{v} \times \vec{\omega}$ to $\vec{F}_b$, $\vec{F}_C$ and $\vec{F}_\nu$, respectively. Turbulence forms when ∇B is negligible and Fr, Ro, Re and all other such dimensionless ratios are greater than critical values, giving

$$\frac{\partial \vec{v}}{\partial t} \approx \vec{v} \times \vec{\omega} \tag{2}$$

from Equation (1). Fluid particles are accelerated in directions perpendicular to both the velocity and vorticity, which are in opposite directions on opposite sides of a shear layer. Because $\vec{v}$ is zero at the shear layer and $\vec{\omega}$gs zero far away, a maximum occurs in both the magnitude of $\vec{v} \times \vec{\omega}$ and the local Reynolds number at distances $\sim L_K$ above and below any free shear layer of age $> T_K$, causing perturbations to be amplified by $\vec{v} \times \vec{\omega}$ forces, as shown in Figure 1. Similarly, the universal critical Re value $\sim 10^2$ is reached at $5L_K$ for a growing laminar boundary layer thickness.

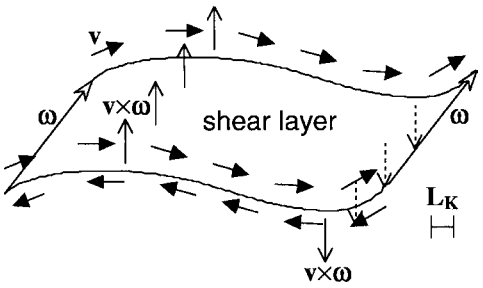

Figure 1. Instability of a shear layer to inertial vortex forces $\vec{v} \times \vec{\omega}$. Turbulent eddies form with Kolmogorov time scale T_K at the Kolmogorov length scale L_K.

We see from Figure 1 that the response of any shear layer to inertial vortex-forces is to roll up into an eddy with diameter $\sim L_K$ in a time $> T_K$. This is the basic inertial vortex force turbulence mechanism. Inertial vortex force turbulence always starts at the Kolmogorov length scale and evolves with the Kolmogorov time scale unless it is constrained by walls or forces larger than $\vec{v} \times \vec{\omega}$.

Therefore, turbulence is defined as an eddy-like state of fluid motion where the inertial vortex forces of the eddies are larger than any other forces that tend to dampen the eddies out. Processes that produce shear layers produce turbulence by the mechanism of Figure 1. Jets, wakes, boundary layers and mixing layers are examples where shear layers are produced at solid surfaces, but shear layers can also form and become turbulent without solid boundaries; for example, in the interior of density stratified fluids, where tilted density interfaces are accelerated by gravitational or other fields.

3. Direction of the Inertial Vortex Force Turbulence Cascade

By our narrow inertial vortex force turbulence definition, turbulence is constrained to cascade from small scales to large. In the turbulence literature, including the classical Kolmogorov and Taylor papers, this unexpected turbulent cascade direction might be termed an "inverse turbulence cascade" or a "spectral back scattering" contrary to the well accepted 1921 Richardson idea that "big whorls have little whorls that feed on their velocity, and smaller whorls have smaller whorls, and so on to viscosity" (for an alternative version of the Richardson turbulence poem, see [12]).

The physical justification for the intrinsic "inverse cascade" in our narrow turbulence definition is that the eddy turnover time is always smaller for small-scale eddies than for large-scale eddies. In a turbulent flow, all eddies influence all other eddies (as well as the irrotational flows which supply the turbulence kinetic energy), so there is feedback in the energy cascade from small scales to large that maintains the universal Kolmogorov equilibrium and homogenizes the flow. The energy cascade in external irrotational flows is from large scales to small, but

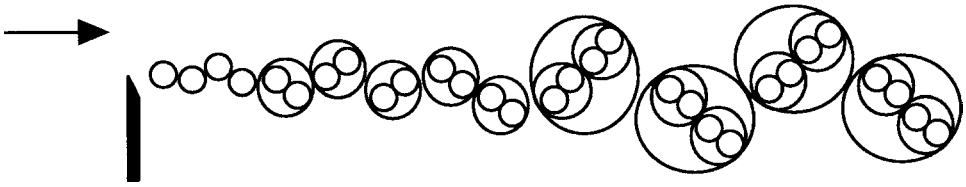

Figure 2. The inertial vortex force turbulence cascade is always from small scales to large. Turbulence induces a random flow of external fluid and kinetic energy from large scales to small, but this is a nonturbulent cascade because irrotational flows have zero $\vec{v} \times \vec{\omega}$ forces.

this is a nonturbulent energy cascade by definition because inertial vortex forces are zero everywhere the vorticity is zero. Rotational turbulent eddies form at the Kolmogorov scale (Figure 1), pair with neighboring eddies, and these pairs pair with neighboring pairs, etc., as shown in Figure 2. Flow over a barrier is given as a generic representation of free shear-layer sources that produce inertial vortex force turbulence.

In Figure 2, the volume of turbulent fluid increases downstream because moving external fluid is entrained to supply the turbulent kinetic energy. The energy cascade induced in the external fluid flow from large scales to small is a broad turbulence definition turbulent cascade because the irrotational external flow is randomized by its turbulent boundary conditions.

4. Definition of Fossil Turbulence

Fossil turbulence is defined as any fluctuation in a hydrophysical field produced by turbulence that is no longer turbulent at the scale of the fluctuation. Familiar examples of fossil turbulence are airplane contrails in the stratified atmosphere, skywriting, clouds, bubble patches from breaking oceanic surface waves, and milk patches in weakly stirred coffee. The time required for a turbulent patch to form by the processes of Figures 1 and 2 is much less than the time required for particle diffusion processes to erase the scars in the numerous hydrophysical fields affected by the turbulence.

Therefore, patches of temperature and salinity microstructure detected in the ocean interior are fossilized by buoyancy forces at their larger scales and persist for long periods [9]. Patches of clear air turbulence are likely to be strongly fossilized at the scale of the aircraft before they are encountered, and are consequently remarkably persistent. Fossil turbulence remnants preserve information about previous active turbulence events that may be difficult or impossible to recover otherwise [12].

5. The First Turbulence and the First Fossil Turbulence

Physics describes small-scale structure using quantum mechanics (QM) and large-scale structure using Einstein's equations of general relativity (GR). However, both

of these theories break down at the Planck-scale initial instant and singularity of the big-bang [16]. The current best hope of reconciliation is provided by multi-dimensional superstring theory (MS) [15]. Gravity is not included in the tensor and scalar fields of standard wave-particle-physics theory, and particles other than black holes do not emerge naturally from Einstein's theory of gravity. There is no currently accepted theory of QGD that provides a quantitative, or even qualitative, description of the first stages of the universe. However, powerful clues constrain QGC theories to the very high temperatures and very small length and time scales indicated physically (from GR, QM and MS) and by dimensional analysis based on light speed c, Planck's constant h, Newton's constant G and Boltzmann's constant k; that is, the Planck scales. A readable summary of cosmological physics is given by Peacock [22]. Remarkably, the concept of a turbulence beginning at Planck scales has been neglected in previous QGD modeling.

According to the present model of the hot big-bang universe, space-time energy emerges from the vacuum spontaneously at Planck scales because a slight possibility of such an event is allowed by Heisenberg's uncertainty principle, where the uncertainty of the energy of a particle ΔE multiplied by the uncertainty of its time of existence Δt is greater than or equal a constant h termed the Planck constant. The Planck mass $m_P = (ch/G)^{1/2}$ is found by equating the Compton wavelength $L_C = h/mc$ of a particle with mass m to the Schwarzschild radius $L_S = Gm/c^2$ of a black hole, where c is the speed of light and G is Newton's gravitational constant. The Planck entropy S_P is equal to the Boltzmann constant k, and gives a minimum black hole specific entropy $s_P = S_P/m_P$, maximum black hole temperature $T_P = (c^5h/Gk^2)^{1/2}$, and minimum black hole evaporation time $t_P = (hG/c^5)^{1/2}$ [15]. Grand unified (GUT) force theories suggest all basic forces of nature (weak, strong, electromagnetic, gravity and now perhaps the inertial vortex force) are equivalent at the Planck–GUT temperatures (10^{32} to 10^{28} K) and are quantized by vibrations of complex string-like objects at Planck scales.

This simplicity of Planck-scale conditions permits a high Reynolds number turbulence and turbulent mixing interpretation for the quantum gravitational dynamics (QGD) epoch of the big-bang. Figure 3 gives the Heisenberg, Compton and Schwarzschild equations, with fundamental constants, Planck m, L, t and T scales and the Planck parameters of the first turbulence. Substituting the Planck viscosity $\nu_P = c^2 t_P$ and Planck dissipation rate ε_P (Figure 3) into the definitions of the Kolmogorov length and time scales gives $L_K = L_P$ and $T_K = t_P$. The Planck thermal diffusivity $\alpha_P = c^2 t_P$, so the Batchelor scale $L_B = (\nu/\alpha^{-1/2} L_K$ also equals L_P, where ν/α is the Prandtl number $Pr_P = 1$. The Heisenberg uncertainty relation given on the first line of Figure 3 has an equal sign corresponding to the highly improbable, reversible, production by quantum tunneling of a Planck mass particle and Planck mass antiparticle. This represents the necessary condition to trigger the big-bang and the formation of the universe within currently understood physics. The Planck mass, length, time and temperature scales were found by dimensional analysis from the fundamental constants c, h, G and k. Planck energy, power,

$$h = \Delta E \times \Delta t = E_P t_P$$

$$L_{Compton} = h/mc = L_{Schwarzschild} = Gm/c^2$$

$$\text{when } m = m_P = [ch/G]^{1/2}$$

$c = 3\times10^{8}$ m s^{-1} $\quad m_P = [ch/G]^{1/2} = 2.12\times10^{-8}$ kg

$h = 1.05\times10^{-34}$ kg m^2 s^{-1} $\quad L_P = [hG/c^3]^{1/2} = 1.62\times10^{-35}$ m

$G = 6.67\times10^{-11}$ m^3 kg^{-1} s^{-2} $\quad t_P = [hG/c^5]^{1/2} = 5.41\times10^{-44}$ s

$k = 1.38\times10^{-23}$ kg m^2 s^{-2} K^{-1} $\quad T_P = [c^5h/Gk^2]^{1/2} = 1.40\times10^{32}$ K

$E_P = [c^5h/G]^{1/2} = 1.94\times10^{9}$ kg m^2 s^{-2}

$P_P = c^5/G = 3.64\times10^{52}$ kg m^2 s^{-3}

$\varepsilon_P = [c^9/hG]^{1/2} = 1.72\times10^{60}$ m^2 s^{-3}

$s_P = [k^2G/ch]^{1/2} = 6.35\times10^{-16}$ m^2 s^{-2} K^{-1}

$\rho_P = c^5/hG^2 = 5.4\times10^{96}$ kg m^{-3}

$F_{GP} = Gm_P^2/L_P^2 = 1.1\times10^{44}$ kg m s^{-2}

$$[\vec{v}\times\vec{\omega}]_P = g_P = [c^7/hG]^{1/2} = 5.7\times10^{51} \text{ m s}^{-2}$$

Figure 3. Planck scales and Planck parameters of the first turbulence.

viscous dissipation rate, specific entropy, density and gravitational force scales of Figure 3 can also be derived by combinations of m_P, L_P, t_P and T_P. For example, the Planck inertial–vortex force per unit mass $[\vec{v} \times \vec{\omega}]_P = L_P/t_P^2$ equals the Planck gravitational force per unit mass $g_P = F_{GP}/m_P = [c^7/hG]^{1/2} = 5.7 \times 10^{51}$ m s^{-2} (Figure 3 bottom line). This suggests the fundamental nonlinear centrifugal force $\vec{v} \times \vec{\omega}$ of our narrow turbulence definition mechanism may arise to balance gravity when Planck particles and antiparticles, which are extreme Schwarzschild black-holes (nonspinning black holes with the minimum possible mass), interact to form the first quantum state: a spinning Planck-particle pair forming an extreme Kerr black-hole (spinning black hole with minimum possible mass).

Electron–positron pair production and positronium formation is a well-documented analogous process known to occur at lower temperatures in supernovae. The Schwarzschild metric of nonspinning black holes has been known since 1916, and the Kerr metric of spinning black holes has been known since 1963 [22] (p. 51–60). In our BBT model, Kerr black holes are capable of Hawking radiation (Planck pair production at their event horizon) with 42% efficiency for prograde collisions [22] (p 61), which produces competing Planck inertial vortex and gravitational forces and the irreversible transfer of angular momentum and energy to larger scales that drives the BBT.

Once the first Planck particle and antiparticle emerge, their enormous temperatures increase the probability of more particle pairs forming nearby, causing and permitting the irreversible turbulent cascade to larger and larger scales, and huge negative Planck—Reynolds stresses $(c^{13}h^{-3}G^{-3})^{1/2} \sim 10^{121}$ m^{-1} s^{-2}, that form the universe in our present BBT model. Negative pressure produces space-time energy from GR. Random interactions between particles and rotating pairs of particles cause larger scale aggregations of pairs with the same rotational sense, just like the

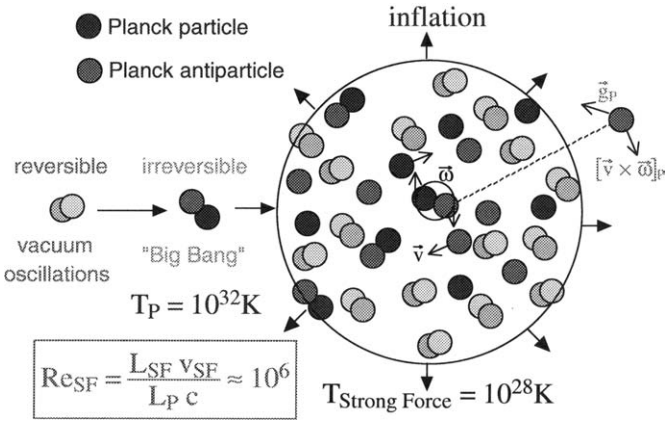

Figure 4. Physical processes of the first turbulence. Reversible vacuum oscillations at Planck scales have a finite probability of forming a Planck particle–antiparticle pair, which can trigger irreversibilities and the formation of the universe. Quantized rotation states (extreme Kerr black-holes, center) can form and produce inertial vortex forces (upper right) that balance gravity, diffuse the spin, slow the annihilation, and homogenize the velocity and temperature fluctuations by turbulent eddy formation and mixing until the strong-force freeze-out (GUT) temperature is reached. Exponential inflation of space caused by the negative Reynolds stress, viscous stress, and possibly false vacuum pressures [16] then fossilize the turbulent temperature field by expansion beyond the scale of causal connection *ct*.

turbulence cascade of Figure 2. Entropy production resulting from this turbulent mixing of velocity and temperature fluctuations in the initial expanding universe is equivalent to entropy production from viscous and temperature dissipation rates ε and χ in less exotic turbulent mixing flows, so that the temperature spectrum ϕ_T should depend only on these rates and the wavenumber k, giving $\phi_T = \beta\chi\varepsilon^{-1/3}k^{-5/3}$ by dimensional analysis with β a universal constant of order one as first shown by Corrsin and Obukhov. Figure 4 illustrates the mechanism.

The entropy production of the hot BBT universe is remarkably small, only about 10 J/K corresponding to the entropy produced by boiling a milligram of water, but this small amount was crucial to the beginning universe which lacked other sources of irreversibility. Most of the entropy of the present universe was produced after inflation, and after the free quarks of the quark–gluon plasma condensed to form hadrons (protons, mesons). Hadrons formed the light elements at the much lower temperatures and later times of the quantum chromo dynamics (QCD) and quantum electro dynamics (QED) epochs.

Because the temperatures of the QGD epoch are too high for small particles to exist, momentum transport is only by short-range Planck particle interactions, giving small kinematic viscosities $\nu_P \approx cL_P$ and large Reynolds numbers $Re = vL/cL_P$ at scale L with velocity $v \approx (2kT)^{1/2}$. According to inflation theory [16], the big-bang cascade terminates when temperatures decrease to the strong-force freeze-out (GUT) temperature $T_{SF} = 10^{28}$ K at time 10^{35} sec, when quarks and

gluons form, with $L = L_{SF} = 10^8 L_P$, $v_{SF} = 10^{-2}c$, and Reynolds number or order 10^6 as shown in Figure 4. The only heavy particle stable in the temperature range $T_P > T > T_{SF}$ is the magnetic monopole with mass about $10^{-2}\, m_P$. Guth found that the lack of observed magnetic monopoles implies an inflationary epoch between time $t = 10^{-35}$ and 10^{-33} s, driven by the equivalent of antigravity forces from a false vacuum negative pressure. During inflation (by a factor of about 10^{25}) the Planck scale fluctuations at 10^{-35} m were stretched to 10^{-10} m, the strong force scale fluctuations at $ct_{SF} = 3 \times 10^{-27}$ m were stretched to 3×10^{-2} m, and geometry was flattened to a nearly Euclidian state at large scales. All the temperature fluctuations of the first turbulence are stretched by this exponential inflation of space to scales much larger than the horizon scale $L_H = ct$ of 3×10^{-25} m existing at the end of the inflation epoch 10^{-33} s, producing the first fossil–temperature turbulence. The expected spectrum for high Reynolds number turbulent temperature fluctuations is the universal Corrsin–Obukhov form $\phi_T = \beta \chi \varepsilon^{-1/3} k^{-5/3}$, where k for the first turbulence is in the range $1/L_{H_{SF}} > k > 1/L_P = 1/L_B$.

Since the formation of quark–gluon plasma marks the end of the QGD epoch, the negative pressure of gluon-viscous forces provides an additional mechanism to drive inflation besides the negative pressures of turbulent Reynolds stresses and the Guth false vacuum. The false vacuum has the important property that its energy density is constant during inflation [16]. Gluons have zero mass and provide bulk viscosity ($c^2 t$) and negative pressures during inflation. Similarly, photons give large Thomson scattering viscosities at the lower temperatures of the plasma epoch, where photon-viscous forces prevent primordial plasma turbulence and inhibit gravitational structure formation until 10^{12} s (30,000 yr) after the big-bang [11, 13].

After inflation, the fossil-temperature turbulence (fossil-curvature turbulence and fossil-vacuum turbulence) fluctuations continue to stretch with the expansion of the universe, following the Einstein GR equations. Fossil Planck scale fluctuations reenter the horizon first because they have the smallest scales, but not until the universe has cooled to the electoweak freeze-out temperature so that radiation in the form of neutrinos and photons with mean free paths much larger than the electron separations provide viscosities sufficient to damp out any turbulence [13]. Because nuclear reactions are very sensitive to temperature, the temperature fossils of the first turbulence imprint the mass density and species concentrations of light elements formed by nucleosynthesis when the first protons, electrons, neutrons and alpha particles form before $t = 10^2$ s [32], converting the temperature fossil turbulence patterns to density and concentration fossil turbulence. Further cooling decreases the neutrino-electron scattering cross-section to negligible levels. Thus, the universe becomes completely transparent to all neutrino species after about 10^2 s [31], producing a cosmic neutrino radiation background picture of the universe at this neutrino decoupling time that may some day be observed when high resolution neutrino telescopes are invented.

Photon viscosity values produce viscous gravitational scales larger than the horizon scale L_H until just before the time of first structure at 10^{12} s [11], when the proto-supercluster mass of 10^{47} kg just matches the horizon mass $L_{H^3\rho}$, where ρ is the density computed from GR theory [31]. Rapid diffusion of the neutrino-like nonbaryonic dark matter fills the proto-supercluster voids, proto-cluster voids and proto-galaxy voids formed in the plasma epoch, reducing gravitational driving forces and arresting further structure formation until after the plasma-gas transition time 10^{13} s (300,000 yr), when the temperature was about 3000 K [13]. At that time the first atoms formed and photons decoupled from electrons, giving the CMB image of the universe that we observe today, redshifted a factor of 1100 by the expansion of the universe into the microwave bandwidth from the original white-hot visible frequencies. Are there any remnants of BBT imprinted on the CMB?

6. Discussion

High resolution maps and spectra of CMB temperature fluctuations have recently been obtained from telescopes carried by balloons to altitudes above atmospheric interference, extending the 1989 Cosmic Background Experiment (COBE) space telescope observations to smaller scales and higher precision. Hu [17] compares a collection of spectral points to various standard cold-dark-matter (CDM) acoustical models, and the present turbulence model is compared to these in Figure 5. Predictions and interpretations of CDM models and the present theory diverge at all wavenumbers. From BBT theory, the statistically significant COBE point on the left (unexplained by CDM theory and missing from the Hu [17] Figure) is interpreted as the fossil –strong force (GUT) horizon scale L_{HSF} stretched by a factor of 10^{50}. The COBE data point is precisedly reconfirmed by WMAP measurements (triangles).

The commonly assumed Harrison–Zel'dovich $k^2\phi_T$ dissipation spectral form [21] is flat with a constant (unspecified) scale-independent temperature fluctuation level $|\delta T|$. This form is inconsistent with the CMB observations of Figure 5. "Tilted" forms have decreasing tails [17] for large k and large Legendre multipole index l. These droop sharply by diffusive damping from the CDM assumption that the temperature fluctuations are acoustic oscillations of plasma trapped in CDM halos.

Standard CDM cosmologies suggest such acoustic oscillations account for the dominant acoustic peak in Figure 5 at $k \sim 220$ and length scale $ct/3^{1/2}$ smaller than the $k \sim 20$ plasma-gas horizon scale L_{HG}, where $c/3^{1/2}$ is the sound speed in the plasma and $t = 10^{13}$ s. COBE (pale), BOOMERanG (dark), MAXIMA (white) and cosmic background imager (CBI) (black; Pearson et al. [23]) data all confirm this acoustic spectral peak. However, such an acoustic peak is better explained as the super-galaxy cluster void fragmentation scale starting at 10^{12} s when the horizon mass matches supercluster and Schwarz viscous mass values [11]. The amplitude $\delta T/T \sim 10^{-4}$ is appropriate for gravitational voids. These grow as rarefaction waves

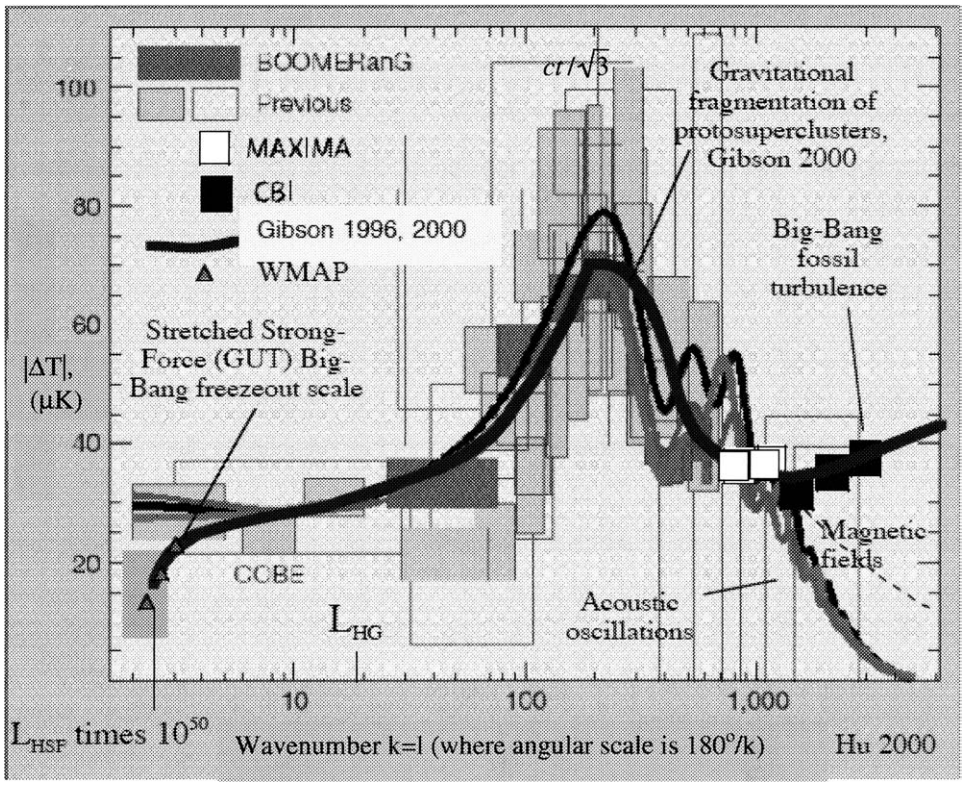

Figure 5. Measured cosmic microwave background (CMB) temperature gradient power spectra ($\Delta T = [k^2\phi]^{1/2}$, μK) compared to CDM acoustical models and the Gibson 1996, 2000 interpretation as plasma fragmentation and big-bang fossil turbulence $\sim k^{1/6}$ ($k = $ l).

limited to sonic speeds and aided by the expansion of the universe. The amplitude is much too large for weakly driven sonic oscillations in this superviscous primordial plasma [13, 14]. CDM acoustic oscillation models cut off sharply for $k > 1000$ due to thermal diffusivity, contrary to the CBI data. The peak at $k \sim 220$ (wavelength 3×10^{21} m) is interpreted as 10^{46} kg plasma fragmentation at 10^{12} s (30,000 yr). Subramanian and Barrow [28] propose a tangled magnetic field explanation (dashed line) for the observed small scale CMB temperature anisotropies above the thermal diffusion cut-off, based on upper limit primordial field strength estimates of Barrow et al. [1].

In Figure 6 (dashed box) the bump marked BOOMERANG represents the prominent peak of Figure 5. The peak occurs at a wavelength $\lambda = ct/3^{1/2}$ corresponding to the sound speed of the plasma epoch, where c is the speed of light, which has been taken by several authors to be evidence that the peak represents sonic oscillations of the plasma in CDM "halos." However, plasma sonic oscillations would be strongly damped by photon-viscous forces due to Thomson scattering of photons with electrons that are strongly coupled to ions by electric forces, and that

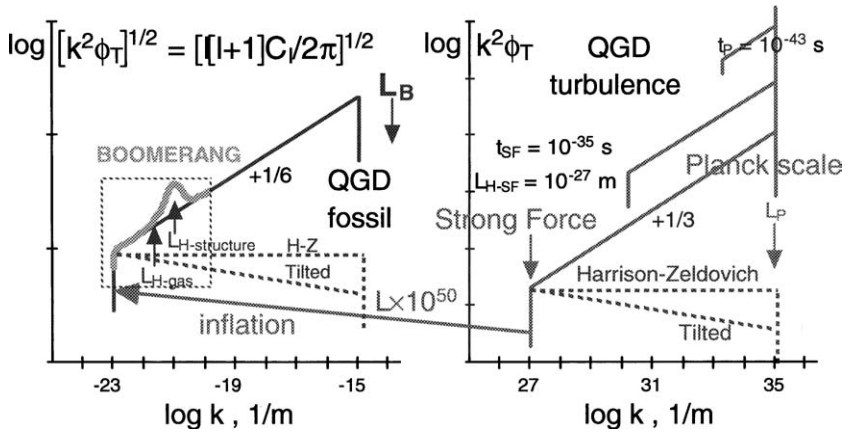

Figure 6. Dissipation spectra for QGD temperature fluctuations. On the right, the present theory predicts turbulent mixing spectral forms that peak at the smallest scale, compared to flat Harrison–Zel'dovich and Tilted forms that peak at the largest scale. A schematic version of the fossilized spectra are shown on the left, after inflation by 10^{50} as indicated by observations in Figure 5 (box). All fluctuations are larger than the Batchelor scale of diffusive damping L_B of about 10^{14} m for ions in the plasma.

the spectral peak of Figure 5 represents an earlier, smaller, horizon scale $L_{H\text{-}structure}$ of proto-galaxy supercluster voids. No powerful cosmological sound source exists to produce such a strong sonic peak, with $\delta T/T \approx 10^{-4}$. CDM clumping is a misconception. Such weakly diffusional matter can fragment only at diffusional scales much larger than the plasma horizon ct for $t < 10^{13}$ s [13].

Measured δT/T $\sim 10^{-5}$ fluctuations are too small to be consistent with strong turbulence in the plasma, but are too large to be caused by sonic fluctuations in this super-viscous fluid with no sonic sources. No diffusive cutoff is expected at high frequencies because the fluctuations should reflect fossil-density turbulence created by nucleosynthesis triggered by BBT remnants. Species density fluctuations have much smaller diffusivities than temperature. Drooping at large k is likely from undersampling errors when only a small fraction of the sky is sampled. Strong intermittency can be expected at small scales for high Reynolds number fossil turbulence.

The suggested interpretations of the observations of Figure 5 are shown schematically in Figure 6, where spectral forms are extended by five decades to the fossilized turbulent Planck scale. If a QGD fossil turbulence spectrum were used with the sonic standard model predictions instead of the Tilted forms, the higher order sonic peaks would become even more inconsistent with the data and the interpretation of the primary peak as a sonic oscillation even less tenable. Higher resolution, higher precision CMB observations may resolve the contradictory predictions in Figures 5 and 6. Gibson [11, 13], suggests the peak reflects the first gravitational formation of structure in the plasma epoch, contrary to the [18] sonic criterion for gravitational structure formation.

The Jeans [18] criterion follows from a linear perturbation analysis of the inviscid Euler momentum equations with gravity, reducing the stability problem to one of gravitational acoustics. By the Jeans theory, sound waves are unstable in a gas of density ρ if the time L/V_S required to propagate a wavelength L at sound speed $V_S$is greater than the time required for gravitational freefall $(\rho G)^{-1/2}$. Density fluctuations smaller than the Jeans scale $L_J = V_S(\rho G)^{-1/2}$ are assumed to be gravitationally stable in standard cosmological models, where G is Newton's gravitational constant (Figure 3).

However, Gibson [11, 13] suggest that viscous, turbulent, and other forces may also set length scale criteria for gravitational structure formation smaller or larger than L_J. Because the horizon scale L_H in the plasma epoch is always smaller than L_J, standard cosmological models such as Weinberg [31], Silk [27], Kolb and Turner [19], Peebles [24], Padmanabhan [21] and Rees [25] assume that no gravitational structures can form. The Jeans criterion is invalid during the plasma epoch, but from heat transfer considerations applies briefly in the gas epoch when protogalaxies fragment to form Jeans-mass 10^{36} kg proto-globular star clusters (PGCs). Diffusive Schwarz scales $L_{SD} = (D^2/\rho G)^{1/4} > ct$ were too large to permit "cold dark matter" clumping of any weakly collisional nonbaryonic dark matter (with large diffusivity D) in the plasma epoch. Viscous and turbulence forces determine gravitational structure formation when either the viscous Schwarz scale L_{SV} or the turbulent Schwarz scale L_{ST} become smaller than L_H, where $L_{SV} = (\gamma\nu/\rho G)^{1/2}$, $L_{ST} = \varepsilon^{1/2}/(\rho G)^{3/4}$, γ is the rate of strain of the gas with density ρ and kinematic viscosity ν and ε is the viscous dissipation rate [11].

As mentioned previously, this occurred at about $t = 10^{12}$ s, or 30,000 yr, so supercluster masses were the first gravitational structures to form, rather than the last as assumed in standard cosmological models. Thus the spectral peak of Figure 5 is likely not sonic but due to gravitational structure formation nucleated by the fossil density fluctuations from the first turbulence at viscous-gravitational and turbulent-gravitational scales in the plasma as soon as these Schwarz scales became smaller than L_H [13].

7. Structure Function Coefficients and Extended Self-Similarity of the CMB

Bershadskii and Sreenivasan [3] have computed structure function ζ_p and extended self similarity (ESS) coefficients of filtered CMB temperature anisotropy data (www.hep.upenn.edu/∼xuyz/qmask.html, [30]) from various telescopes on space satellites as well as on the Earth surface, where ζ_p are power law coefficients for pth-order structure functions $|\Delta T|_r^p \approx r^{\zeta_p}$ for fluctuations of hydrophysical fields like T with separation r [2]. Results of their computations are shown in Figure 7 compared to $\zeta_p$values from flows that are nonturbulent by our definition.

The best known velocity structure function relation was predicted for high Reynolds number turbulent (HRT) velocity differences by Kolmogorov in 1941 using his second universal similarity hypothesis for $p = 3$ giving $\zeta_p = 1$ by

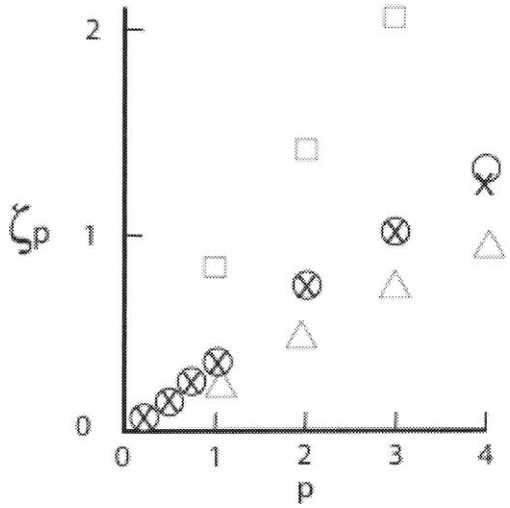

Figure 7. Structure function coefficients for CMB temperature anisotropies [3] agree precisely with those measured for high Reynolds number turbulence (x). Nonturbulent solar wind (triangles) and Reyleigh–Benard convection (squares) $\zeta_p$gvalues, [2], Table 1, do not.

dimensional analysis. For $p = 2$ one finds $\zeta_p = 2/3$ by the same method, corresponding to the $-5/3$ inertial subrange of universal HRT velocity and turbulent mixing spectra. These values are shown in Figure 7 for HRT and the CMB temperature anisotropies, but not for the MHD fluctuations of the solar wind or the viscous and buoyancy affected low Reynolds number fluctuations of Reyleigh–Benard convection. It will be interesting in the future to compute ESS and coefficients for random sonic fields, which are unlikely to match the HRT and CMB coefficients unless the sound is driven by turbulence.

Bershadskii and Sreenivasan [3] selected a range of separation distances r for their structure function calculations corresponding to the smallest noise level acoustic peak region of the CMB data [30]. As shown in Figure 7, the ζ_p coefficients are identical to those for strong turbulence and differ significantly from $\zeta_p$goefficients found in nonturbulent random flow systems such as the solar wind (magnetohydrodynamic and viscous forces) and thermal convection (buoyant and viscous forces, [2]). Tests were made of ground based versus space telescope CMB coefficient measurements. No change was found in the results, ruling out the possibility that these "fingerprints of Kolmogorov" (quoting Bershadskii, personal communication [3]) could somehow reflect atmospheric turbulent mixing rather than a primordial high Reynolds number-turbulence origin as proposed here. Wilkenson Microwave Anisotropy Probe (WMAP) CMB data also support indications of a strong turbulence and departures from Gaussianity [4, 14]. Assuming the signature is that of strong primordial turbulence, the most likely time of the turbulence is the big-bang. High levels of radiation viscosity produce weak or nonturbulent Re values in other epochs, not the Re $\sim 10^6$ values inferred for BBT in Figure 4.

8. Conclusions

The chaotic QGD epoch at Planck scales in the beginning of the universe satisfies our definition of turbulence and the small-to-large direction of the turbulent cascade. Inertial vortex forces that define and drive ordinary turbulence are identified with an efficient Hawking radiation of energy and angular momentum that results when nonspinning Planck-scale extreme Schwarzschild black-holes achieve prograde orbits about Planck-scale spinning extreme Kerr black-holes. The Planck inertial vortex force matches the Planck-scale gravitational force and produces the vorticity, Planck gas, BBT and irreversibility required to form the universe. Electromagnetic, weak, strong, gravitational and inertial vortex forces are equivalent at Planck temperatures 10^{32} K, where only Planck particles, Planck antiparticles and Planck–Kerr particles can exist. These particles interact at a Planck length-scale $L_P = 10^{-35}$ m that is less than the expanding universe horizon scale $L_H = ct$. Only Planck particle–particle viscosities $L_P c$ can transmit momentum, thus giving large Reynolds numbers $L_{SF} v_{SF} / L_P c$ up to 10^6 in the BBT before the universe cools to the GUT strong-force freeze-out temperature 10^{28} K. Quark–gluons then appear with long-range forces and a 10^6 larger gluon-viscosity $L_{SF} v_{SF}$ that damps the BBT, with $L_{SF} = 10^8 L_P$ and $v_{SF} = 10^{-2}\, c$.

Gluon viscosity gives negative pressures that combine with negative pressures of BBT Reynolds stress and the Guth false vacuum to produce exponential inflation of space from Planck to atomic dimensions according to Einstein's GR equations. Evidence of BBT is provided by the CMB data. High wavenumber CBI spectral data in Figure 5 are significantly nonzero showing the spectrum is not acoustical temperature but more likely fossil BBTH–He density. The ζ_P coefficients of Figure 7 show that the statistical distribution of primordial CMB temperature anisotropies are in good agreement with those of high Reynolds number turbulence to fourth order. This supports the present BBT scenario, since no turbulence in the viscous plasma epoch should have high Reynolds numbers.

It is suggested from the CMB temperature anisotropy spectrum of Figure 5 that remnants of hot BBT at the strong-force freeze-out scale $L_{SF} = 3 \times 10^{-27}$ m have been inflated by a factor of 10^{50} to scales ten times larger than the gas horizon wavelength $\lambda_{HG} = 3 \times 10^{22}$ m existing at the time of the plasma to gas transition, and that BBT must have occurred before inflation to explain observed uniform fluctuations independent of direction on the sky but outside each other's horizons. If the dominant spectral peak at $ct/3^{1/2} = 3 \times 10^{21}$ m wavelength has been stretched by a factor of 10^3 corresponding to the gas redshift $z = 1100$, then its scale matches the observed 10^{24} m scale of supervoids and superclusters and confirms our interpretation that the peak is due to the first gravitational structure formation at 10^{12} s by expansion of proto-galaxy supercluster voids at the speed of sound $c/3^{1/2}$ for most of the CMB time t of 10^{13} s, and that subsequent proto-galaxy cluster voids and proto-galaxy voids expand with the expanding universe after fragmentation [14, Figs. 5, 6]. Galaxy-cluster mass densities and galaxy mass

densities ρ have expanded more slowly due to gravity and friction, starting from the initial baryonic value of $\rho_0 = 10^{-17}$ kg m^{-3} existing at 10^{12} s. This fossil density ρ_0 is retained by luminous globular star clusters and dark proto-globular star clusters [11].

Galaxy mass densities rarely increase by collapse or accretion processes. Some evidence of 10^{48} kg supercluster complexes has been reported on the 10^{25} m scales of present stretched strong force scales L_{SFnow}, within the present horizon $L_H = 10^{26}$ m [29]. The most distant galaxies have measured redshifts $z > 4$ and are already strongly clustered, contrary to standard cold-dark matter hierarchical clustering models where clustering occurs at the last rather than the first stages of gravitational structure formation.

Thus, Kolmogorov universal similarity of the velocity fluctuations and Corrsin–Obukhov–Batchelor universal similarity of the temperature and chemical species fluctuations in the expanding, cooling, hot BBT universe are expected with maximum amplitude of the CMB temperature gradient spectrum occurring at the inflated Planck length scale source of the temperature fluctuations $10^{50} L_P = 3 \times 10^{15}$ m. Inflation of space at the strong-force freeze-out temperature fossilized eight decades of turbulent temperature fluctuations by stretching beyond the horizon scale of causal connection, and these provided chaotic seeds for nucleosynthesis and gravitational structure formation after they reentered the horizon. Baryonic (ordinary) matter concentrations preserve the fossil temperature turbulence patterns formed in the QGD epoch as density and light element concentration fluctuations, which reappear as temperature fluctuations in the CMB by the gravitational Sachs–Wolfe red-shift mechanism.

Future CMB measurements are anticipated with improved resolution, precision and broader sky coverage to further test the inferred CMB inflation factor 10^{50}, and the increasing spectral levels at small scales predicted by the present BBT theory versus the drooping sonic forms, Figure 5. Magnetic field explanations of the high wave-number departures [28], should be investigated at very large wave-numbers. Big-bang fossil turbulence CMB spectra increase for several decades with wave-number, but tangled magnetic field spectra decrease (Figure 5). Gravity waves detected by the Laser Interferometer Space Antenna (LISA) and other ground and space based Gravity Wave telescopes may also contribute to understanding the primordial turbulent beginnings of the universe [6].

References

1. Barrow, J.D, Ferreira, P.G. and Silk, J., Constraints on a primordial magnetic field. *Phys. Rev. Lett.* **78** (1997) 3610.
2. Benzi, R., Biferale, L., Ciliberto, S., Struglia, M.V. and Tripiccione, R., Generalized scaling in fully developed turbulence. *Physica D* **96** (1996) 162–181.
3. Bershadskii, A. and Sreenivasan, K.R., Multiscaling of cosmic microwave background radiation. *Phys. Lett. A* **299** (2002) 149–152.

4. Bershadskii, A. and Sreenivasan, K.R., Extended self-similarity of the small-scale cosmic microwave background anisotropy. *Phys. Lett. A* **319** (2003) 21–23.
5. Brandenburg, A., Enqvist, K. and Olesen, P., Large-scale magnetic fields from hydromagnetic turbulence in the very early universe. *Phys. Rev. D* **54** (1996) 1291–1300.
6. Dolgov, A.D., Grasso, D. and Nicolis, A., Relic backgrounds of gravitational waves from cosmic turbulence. *Phys. Rev. D* **66** (2002) 103505.
7. Gibson, C.H., Fine structure of scalar fields mixed by turbulence I. Zero-gradient points and minimal gradient surfaces. *Phys. Fluids* **11** (1968) 2305–2315.
8. Gibson, C.H., Fine structure of scalar fields mixed by turbulence II. Spectral theory. *Phys. Fluids* **11** (1968) 2316–2327.
9. Gibson, C.H., Internal waves, fossil turbulence, and composite ocean microstructure spectra. *J. Fluid Mech.* 168 (1986) 89–117.
10. Gibson, C.H., Kolmogorov similarity hypotheses for scalar fields: Sampling intermittent turbulent mixing in the ocean and Galaxy, In: *Turbulence and Stochastic Processes: Kolmogorov's Ideas 50 Years On*, Proceedings of the Royal Society London, Ser. A, V434 N1890 (1991) pp. 149–164,.
11. Gibson, C.H., Turbulence in the ocean, atmosphere, galaxy, and universe, *Appl. Mech. Rev.* **49** (5) (1996) 299–315.
12. Gibson, C.H., Fossil turbulence revisited. *J. Mar. Syst.* **21** (1–4) (1999) 147–167.
13. Gibson, C.H., Turbulent mixing, diffusion and gravity in the formation of cosmological structures: The fluid mechanics of dark matter. *J. Fluids Eng.* **122** (2000) 830–835.
14. Gibson, C.H., The first turbulent combustion, *Combust. Sci. Technol.* (2004, to be published).
15. Greene, B., *The Elegant Universe*, Norton, NY (1999).
16. Guth, A., *The Inflationary Universe*, Addison Wesley, NY (1997).
17. Hu, W., Ringing in the new cosmology. *Nature* **404** (2000) 939.
18. Jeans, J.H., The stability of a spherical nebula. *Phil. Trans. R. Soc. Lond. A* **199** (1902) 1.
19. Kolb, E.W. and Turner, M.S., *The Early Universe*, Addison Wesley, NY (1990).
20. Leung, P.T. and Gibson, C.H., Turbulence and fossil turbulence in oceans and lakes. *Chin. J. Oceanol. Limnol.* **22** (1) (2004) 1–23.
21. Padmanabhan, T., *Structure Formation in the Universe*, Cambridge University Press, Cambridge, UK (1993).
22. Peacock, J.A., *Cosmological Physics*, Cambridge University Press (2000).
23. Pearson, T.J., Mason, B.S., Readhead, A.C.S., et al., The Anisotropy of the microwave background to $l = 3500$: Mosaic observations with the cosmic background imager. *Astrophys. J.* **591** (2003) 556–574.
24. Peebles, P.J.E., *Principles of Physical Cosmology*, Princeton University Press, Princeton, NJ (1993).
25. Rees, M., *New Perspectives in Astrophysical Cosmology*, Cambridge University Press, UK (2000).
26. Sievers, J.L., Bond, J.R., Cartwright, J.K. and 14 others, Cosmological parameters from cosmic background imager observations and comparisons with BOOMERANG, DASI and MAXIMA, *ApJ* **591** (2003) 599–622 submitted (astro-ph/0205387) (2002).
27. Silk, J., *The Big Bang*, W.H. Freeman and Company, NY (1989).
28. Subramanian, K. and Barrow, J.D., Small-scale microwave background anisotropies arising from tangled primordial magnetic fields. *Mon. Not. R. Astron. Soc.* **335** (2002) L57–L61.
29. Tully, R.B., More about clustering on a scale of 0.1 c. *ApJ.* **323** (1987) 1–18.
30. Xu, Y., Tegmark, M., Oliveira-Costa, A., Devlin, M.J., Herbig, T., Miller, A.D., Netterfield, C.B. and Page, L., Comparing and combining the Saskatoon, QMAP and COBE CMB

maps. *ApJ* preprint submitted (astro-ph/0010552, www.hep.upenn.edu/∼xuyz/qmask.html) (2001).
31. Weinberg, S., *Gravitation and Cosmology: Principles and Applications of the General Theory of Relativity*, John Wiley & Sons, New York (1972).
32. Weinberg, S., *The First Three Minutes*, Basic Books, Inc., Publishers, New York (1977).